



THE CORROSION BEHAVIOUR AND STRUCTURE OF AMORPHOUS AND THERMALLY TREATED Fe-B-Si ALLOYS

R Raicheff, V. Zaprianova, E. Petrova

University of Chemical Technology and Metallurgy, 8 Kl. Ohridski Blvd., 1756 Sofia, Bulgaria

Abstract: The corrosion behaviour of magnetic amorphous alloys $\text{Fe}_{78}\text{B}_{13}\text{Si}_9$, $\text{Fe}_{81}\text{B}_{13}\text{Si}_4\text{C}_2$ and $\text{Fe}_{67}\text{Co}_{18}\text{B}_{14}\text{Si}_1$ obtained by rapid quenching from the melts are investigated in a model corrosive environment of 1N H_2SO_4 . The structure of the alloys is characterized by DTA, SEM, TEM, X-ray and electron diffraction techniques. The dissolution kinetics of the alloys is studied using gravimetric and electrochemical polarization measurements. It is established that the corrosion rate of the amorphous $\text{Fe}_{67}\text{Co}_{18}\text{B}_{14}\text{Si}_1$ alloy is up to 50 times lower than that of $\text{Fe}_{78}\text{B}_{13}\text{Si}_9$ alloy and the addition of cobalt leads to a considerable reduction of the rates of both partial corrosion reactions, while the addition of carbon results only in a moderate decrease (2-3 times) of the corrosion rate. It is also shown that the crystallization of the amorphous $\text{Fe}_{78}\text{B}_{13}\text{Si}_9$ alloy (at 700°C for 3 h) leads to formation of multiphase structure consisting of crystalline phases $\alpha\text{-Fe}$ and $\text{Fe}_3(\text{B},\text{Si})$. After crystallization an increase of the rate of both hydrogen evolution and anodic dissolution reactions is observed which results in a considerable (an order of magnitude) increase of the corrosion rate of the alloy.

1. INTRODUCTION

The amorphous metallic alloys are accepted as perspective materials with valuable magnetic, electrical and mechanical properties. They possess also the necessary preconditions for revealing of high corrosion resistance - homogeneous structure characteristic with absence of grain boundaries, segregations and other defects of the crystalline state.

The amorphous alloys on iron basis containing metalloids Si and B already find application as soft magnetic materials. The substitution of the conventional electrotechnical Si-steels with amorphous Fe-B-Si alloys in the cores of distributing transformers could lead to an increase of the maximum transformed power (up to 60%) and considerable economy of electric power [1-3].

Improvement of the magnetic properties of those alloys may be obtained by addition of carbon or alloying with cobalt as well as by thermal treatment of the alloys [4,5].

The effect of thermal treatment on the electrochemical corrosion behavior of Fe-B-Si alloy is only scarcely studied. The polarization measurements of $\text{Fe}_{77,5}\text{B}_{15}\text{Si}_{7,5}$ in neutral borate solutions are performed and it is pointed out that heating of the alloy at temperatures $650\text{-}700^\circ\text{C}$ leads to some decrease of its ability to passivation [6]. In general, one should expect that a multiphase crystallization of amorphous Fe-B-Si alloys will result in an increase of the corrosion rate as already established for amorphous alloys of the types Fe-Ni-Cr-P-C [7], Fe-Ni-B [8], Ni-P [9] and Ni-Ti [10].

The aim of the present work is to study the corrosion behaviour of amorphous $\text{Fe}_{78}\text{B}_{13}\text{Si}_9$, $\text{Fe}_{81}\text{B}_{13}\text{Si}_4\text{C}_2$ and $\text{Fe}_{67}\text{Co}_{18}\text{B}_{14}\text{Si}_1$ alloys as well as the effect of thermally induced structural changes (crystallization) on the electrochemical corrosion behaviour of amorphous $\text{Fe}_{78}\text{B}_{13}\text{Si}_9$ alloy.

2. EXPERIMENTAL

The samples of amorphous $\text{Fe}_{78}\text{B}_{13}\text{Si}_9$, $\text{Fe}_{81}\text{B}_{13}\text{Si}_4\text{C}_2$ and $\text{Fe}_{67}\text{Co}_{18}\text{B}_{14}\text{Si}_1$ alloys were produced in the form of ribbons (40 μm thick) by rapid quenching from the melts. Samples of the as-quenched $\text{Fe}_{78}\text{B}_{13}\text{Si}_9$ alloy were subjected to heat treatment in evacuated quartz tubing at 700°C for 3 hours.

The structure of the alloys was characterized by XRD (PW1730/10 diffractometer), TEM (EM-400 Philips) and DTA (Paulik apparatus). The XRD measurements were performed using monochromatic $\text{CuK}\alpha$ ($\lambda=1,5478\text{\AA}$) radiation.



The corrosion experiments were carried out in a corrosive environment of 1N H₂SO₄ at room temperature. The dissolution kinetics of the alloys was studied by gravimetric measurements (Sartorius Analytical weights). The average corrosion rates were estimated from the linear approximation of the experimental weight-loss - time curves using an Excel computer program. Polarization measurements were carried out using the potentiodynamic technique (EG&G Princeton Applied Research Potentiostat 263A) at a potential sweep rate of 20 mV/min and a three-electrode cell with a specially designed electrode holder for flat specimens [11]. All potentials were measured with respect to the saturated calomel electrode (SCE).

3. RESULTS AND DISCUSSION

3.1. CORROSION BEHAVIOUR OF AMORPHOUS FE-B-SI BASED ALLOYS

The kinetic curves of dissolution of the amorphous alloys Fe₇₈B₁₃Si₉, Fe₈₁B₁₃Si₄C₂ and Fe₆₇Co₁₈B₁₄Si₁ in 1N H₂SO₄ are shown on Fig.1. The experimental results show that all alloys investigated dissolve actively and the process of dissolution could be approximated to a linear relationship. The steady-state corrosion rates of the alloys calculated from the kinetic curves are shown in Fig.2. As seen the rate of dissolution of Fe₆₇Co₁₈B₁₄Si₁ alloy is much lower in comparison with the rates of Fe₈₁B₁₃Si₄C₂ and especially of Fe₇₈B₁₃Si₉ alloys.

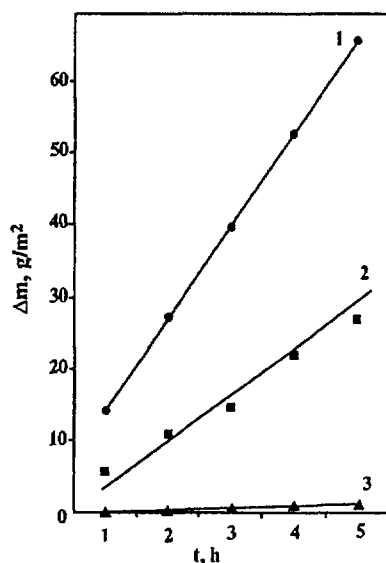


Figure 1: Kinetic curves of dissolution of amorphous Fe₇₈B₁₃Si₉ (1), Fe₈₁B₁₃Si₄C₂ (2) and Fe₆₇Co₁₈B₁₄Si₁ (3) alloys in 1N H₂SO₄

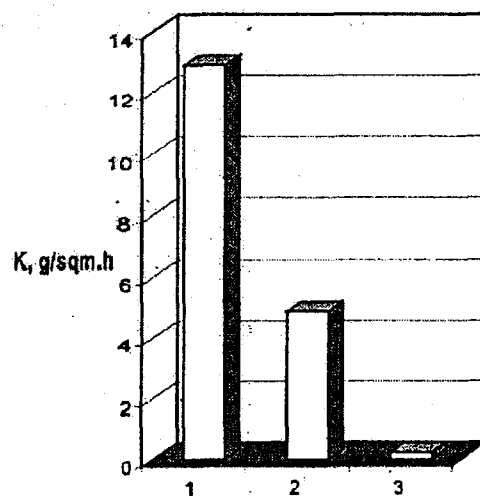


Figure 2: Corrosion rates (K) of amorphous Fe₇₈B₁₃Si₉ (1), Fe₈₁B₁₃Si₄C₂ (2) and Fe₆₇Co₁₈B₁₄Si₁ (3) alloys

Taking Fe₇₈B₁₃Si₉ as a base alloy, the addition of 2% C to the alloy decreases its corrosion rate by a factor of about two. This result seems to be in contrast to the corrosion resistance of crystalline iron alloys at their corrosion with hydrogen depolarization – an increase of the rate of hydrogen evolution reaction and the corrosion rate in acid solutions with increase of the carbon content in the alloy (i.e. the number of cathodically active graphites and carbides inclusions) is usually observed. The present study however shows that there is no such beneficial effect of carbon on hydrogen evolution reaction when it is uniformly distributed in the amorphous matrix. This result is in agreement with the beneficial role of carbon in decreasing corrosion rates of the some other amorphous alloys reported in the literature [12]. The effect of cobalt on the corrosion rate of the alloy is much higher - the alloying of amorphous Fe-B-Si alloy with 18% Co increases its corrosion resistance about 50 times.

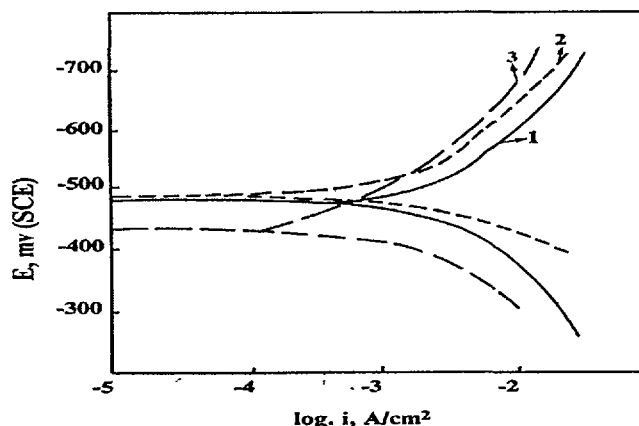


Figure 3: Potentiodynamic polarization curves of amorphous $\text{Fe}_{78}\text{B}_{13}\text{Si}_9$ (1), $\text{Fe}_{81}\text{B}_{13}\text{Si}_4\text{C}_2$ (2) and $\text{Fe}_{67}\text{Co}_{18}\text{B}_{14}\text{Si}_1$ (3) alloys in 1N H_2SO_4

The main results from the electrochemical measurements are illustrated in Fig.3. As it is seen, the effect of alloying with cobalt on the electrochemical corrosion behaviour of the alloy is much more expressed than that of carbon, what is in agreement with the results from weight-loss measurements. Cobalt leads to a decrease of the rate of both partial corrosion reactions-hydrogen evolution and anodic dissolution, thus lowering the overall corrosion rate of the amorphous Fe-B-Si alloy in acid solutions.

3.2. EFFECT OF THERMALLY INDUCED STRUCTURAL CHANGES OF AMORPHOUS $\text{Fe}_{78}\text{B}_{13}\text{Si}_9$ ALLOY ON ITS CORROSION BEHAVIOUR

3.2.1. THERMAL STABILITY

The thermal stability of the amorphous $\text{Fe}_{78}\text{B}_{13}\text{Si}_9$ alloy is studied by differential thermal analysis. The DTA-curve (Fig.4) is characterized by well expressed exothermic peak at 650 °C and a prepeak at 630 °C associated with the two-stepped crystallization of the alloy. The DTA data allows the determination of the parameters of thermal treatment of the alloy.

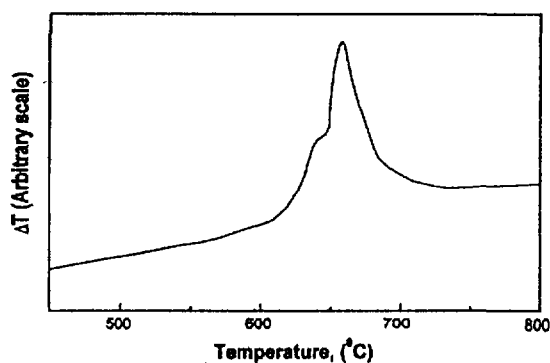


Figure 4: DTA-curve of as-quenched $\text{Fe}_{78}\text{B}_{13}\text{Si}_9$ alloy (heating rate 10°C/min)

3.2.2. CRYSTALLIZATION

The X-ray diffraction patterns of as-quenched and heated at 700 °C $\text{Fe}_{78}\text{B}_{13}\text{Si}_9$ alloy samples are shown in Fig.5. As it is seen, the well formed diffuse halo pattern of XRD diagram for as-quenched sample (curve 1) illustrates the amorphous state of this sample. The thermal treatment of the alloy at



temperature higher than the crystallization temperature results in formation of a multiphase crystalline structure composed of α -Fe and iron borides and silicides - $\text{Fe}_3(\text{B},\text{Si})$ (curve2). The same phases were determine in other investigations [13] on the crystallization of an alloy of the type Fe-Si-B. The transmission electron microscopy observations showed that the microstructure of the alloy after thermal treatment is polycrystalline with an average diameter of the crystals of about 200 nm.

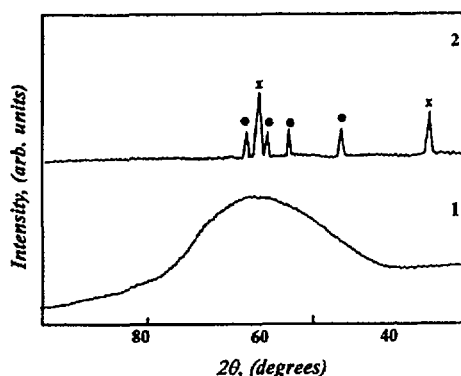


Figure 5: X-ray diffraction patterns for as-quenched (1) and heated (2) at 700°C/3h

3.2.3. EFFECT OF CRYSTALLIZATION ON THE CORROSION BEHAVIOUR OF THE ALLOY

The kinetics curves of dissolution of as-quenched and thermally treated $\text{Fe}_{78}\text{B}_{13}\text{Si}_9$ alloys in 1N H_2SO_4 are shown in Fig.6. The corrosion rate of the crystallized alloy (cf. also Fig.7) is about an order of magnitude higher than that of the amorphous as-quenched alloy. The crystallization of the alloy leads to an increase of the rates of both partial corrosion reactions - hydrogen evolution and anodic dissolution, thus enhancing the overall corrosion rate of the alloy (Fig.8).

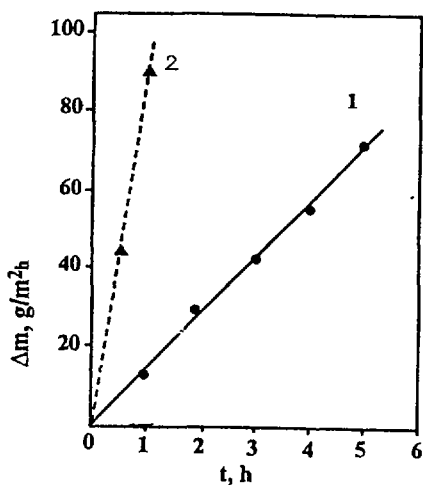


Figure 6: Kinetic curves of dissolution of $\text{Fe}_{78}\text{B}_{13}\text{Si}_9$ amorphous (1) and crystallized (2) alloys in 1N H_2SO_4

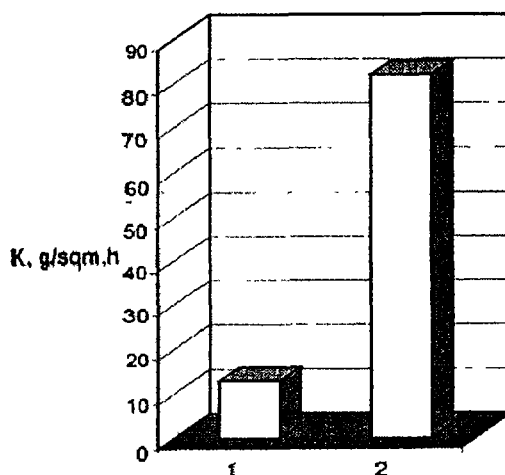


Figure 7: Corrosion rates (K) of amorphous (1) and crystallized (2) $\text{Fe}_{78}\text{B}_{13}\text{Si}_9$ alloys in 1N H_2SO_4



The lower dissolution rate of the amorphous $\text{Fe}_{78}\text{B}_{13}\text{Si}_9$ alloys in comparison with that of the crystallized alloy is obviously related to the features of the amorphous state – a homogenous structure and absence of grain boundaries, dislocations, kink sites and other surface defects characteristic for the crystalline state [7-10,14]. The crystalline phases formed during crystallization ($\alpha\text{-Fe}$ and iron borides and silicides - $\text{Fe}_3(\text{B},\text{Si})$) show a higher catalytic activity for the hydrogen evolution reaction than the amorphous alloy (cf. Fig.8) which is an additional factor for increasing the corrosion rate of the crystallized alloy in acidic environments.

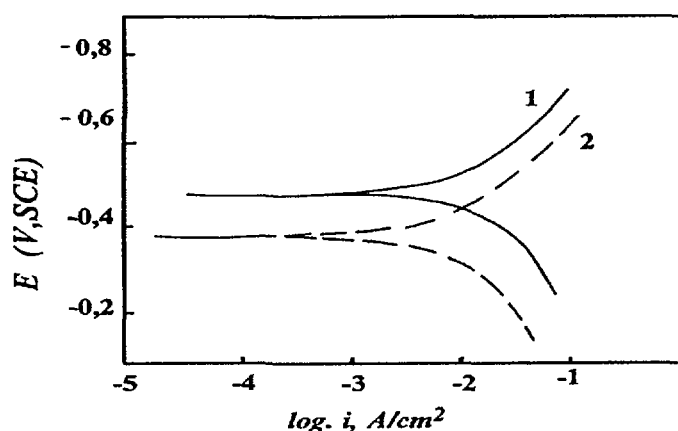


Figure 8: Potentiodynamic polarization curves of amorphous (1) and crystallized (2) $\text{Fe}_{78}\text{B}_{13}\text{Si}_9$ alloys in 1N H_2SO_4

The data in the literature for the electrochemical properties of iron silicides and borides however are largely missing in order to make a quantitative assertion of the mechanism for enhanced corrosion of the crystallized alloy.

4. CONCLUSION

On the basis of the results in the present study the following conclusions could be made:

- (i) The amorphous Fe-B-Si alloys show low corrosion resistance and active anodic dissolution in acidic media. The addition of carbon and especially of cobalt to the amorphous Fe-B-Si alloy however improves considerably its corrosion resistance;
- (ii) The thermal treatment above the crystallization temperature of the amorphous $\text{Fe}_{78}\text{B}_{13}\text{Si}_9$ alloy results in formation of multiphase crystalline structure composed by $\alpha\text{-Fe}$ and iron borides and silicides - $\text{Fe}_3(\text{B},\text{Si})$;
- (iii) The crystallization of the amorphous $\text{Fe}_{78}\text{B}_{13}\text{Si}_9$ alloy leads to an increase of the rates of both partial corrosion reactions - hydrogen evolution and anodic dissolution, thus decreasing considerably the corrosion resistance of the alloy in acidic media.

Acknowledgements

The financial support of Bulgarian NSF under Project № 310/2000 (X-1004) is gratefully acknowledged.

Reference

- [1] F. Lubovsky, "Amorphous Metallic Alloys", Butterworths, London (1983)
- [2] R. Hasegawa, J. Magnetism Magn. Mater. 215-316,240 (2000)
- [3] N. Ershov and V. Kazakov, Stal 5, 62, Russia (1997)
- [4] L. Kanchang and C. Xiaozuqe ,Gongneng Cailiao 29, 315 (1998)



- [5] Magnetic Materials, Honeywell, New Jersey (2000)
- [6] J. Chattoraj, A. Bhattamishira, A. Mitra, Corrosion 49,707 (1993)
- [7] M. Naka, K. Hashimoto, T. Masumoto, Corrosion 36, 679 (1980)
- [8] V. Zaprianova, R. Raicheff, Proc. Intern. Symposium on Glass Problems, IGC, Istanbul, v.2, p.82 (1996)
- [9] V. Zaprianova, R. Raicheff, L. Fachikov, Bulg. Chem. Commun.,27, 162 (1994)
- [10] V. Zaprianova, R. Raicheff, E. Gateff, Cryst. Res. Technol. 33, 425 (1998)
- [11] V. Zaprianova, R. Raicheff, Proc. Eurocorr '91
- [12] M. Naka, K. Hashimoto, T. Masumoto, J. Non- Cryst. Solids, 213 (1988)
- [13] Y. Takahara, N. Narita, Mater. Transac. JIM 41, 981 (2000)
- [14] A. Inone , K. Hashimoto, "Amorphous and Nanocrystalline Materials", Springer,Berlin (2001)